Lasers in Manufacturing Conference 2023

The effect of temporal pulse overlaps to the morphology on stainless steel 304 at ps laser micro structuring.

Munehiro Chijiiwa[a,*], Niklas Berger[a], Mareike Schäfer[a], Peter Mitschang[b], and Johannes A. L'huillier[a]

[a]*Photonik-Zentrum Kaiserslautern e.V., and Research Center OPTIMAS, TU Kaiserslautern, 67663 Kaiserslautern, Germany*
[b]*IVW—Leibniz-Institut fu¨r Verbundwerkstoffe GmbH, Manufacturing Science, 67663 Kaiserslautern, Germany*

Abstract

In this study, for creating a bumpy structure on the thin metal films with low heat accumulation, morphologies at different heat accumulation conditions were examined by changing the time interval between laser pulses (1 µs, 2.5 µs, and 25 µs), applying these with the same spatial pulse overlap. The comparison of morphologies and calculated saturation temperature showed that there are conditions where a bumpy structure is formed, even below the critical saturation temperature for bumpy structures. To discuss the boundary of the growth mechanism of a bumpy structure, which incubation mechanism is dominant at the different time intervals is studied. The analysis from the incubation model showed that for a time interval between pulses of 25 µs, the absorption and no longer the heat accumulation is the dominant factor. The results promote the idea that the boundary of mechanism for forming bumpy structures might be predictable by the incubation model.

Keywords: USP laser; heat accumulation; morphology; incubation effect

1. Introduction

Surface functionalization, especially for wettability control, is expected in many technical applications (Yong et al. 2017; Manoharan and Bhattacharya 2019). Imparting such properties, especially on thin metal surfaces, is expected to have applications in microfluidic channels and medical devices (Berger et al. 2021). For example,

* Corresponding author. Tel.: +49-631-415-5750; fax: +49-631-415-575-10.
E-mail address: munehiro.chijiiwa@pzkl.de.

in the microfluidic channels, when the wall's surface is superhydrophobic (Cassie-Baxter states), an effective sliding of the fluid over the surface occurs instead of being a no-slip boundary condition (Schönecker, Baier, and Hardt 2014).

Due to the possibility of precise heat control during the manufacturing process, USP-laser-micromachining seems to be a promising technique for creating a superhydrophobic state on thin metal film surfaces. In contrast to other technologies, this process works without masks or contacts and can be applied over large areas, even on curved surfaces. It allows the generation of hierarchical structures on the micro- and nanometer scale. Additionally, the ablation process also allows the chemical part of the wettability to be influenced. The wetting properties can also be controlled to a certain extent by the use of process gases or processes such as ultrafast alloying.

There are a variety of laser-induced surface structures, such as laser-induced periodic surface structure (LIPSS) (Martínez-Calderon et al. 2016; Giannuzzi et al. 2019), groove structures (Ahmmed et al. 2015), and bumpy/sponge-like structures (Bauer et al. 2015). To achieve the Cassie-Baxter state, in this study, the bumpy/sponge-like structure is focused on as one of the candidate structures (Sciancalepore et al. 2018).

While when creating some surface structure on a thin metal film surface by laser micro-structuring, one of the concerns is heat accumulation since it can cause bending of the material (Pence et al. 2013).

Therefore, to create a bumpy/sponge-like structure, a manufacturing process with low heat accumulation is needed for microfluidic channel devices.

Regarding the growth mechanism of a bumpy structure, the existing models may be roughly divided into two groups. One growth mechanism is that the structure or debris deposition affects the reflection and absorption of subsequent laser pulses, expanding the previous structure (Zuhlke, Anderson, and Alexander 2013; Ling et al. 2015). Another growth mechanism is that heat accumulation causes grooves to grow through convection mechanisms, then leading to the formation of bumps (Zuhlke, Anderson, and Alexander 2013; Bauer et al. 2015; Fraggelakis et al. 2017; Faas et al. 2018; Nyenhuis et al. 2022). Therefore, to create bumpy/sponge-like structures with low heat accumulation, one needs to know the boundary of the growth mechanism of a bumpy structure and use the growth mechanism without too much heat accumulation.

Regarding the boundary of the growth mechanism of a bumpy structure, some studies suggest that laser fluence is one of the indicators (Zuhlke, Anderson, and Alexander 2013). However, the heat accumulation can be low even if in the high fluence when the pulse repetition rate is low. Thus, the boundary of the growth mechanism of a bumpy structure is not well known.

One of the ideas of the indicator for the boundary of the growth mechanism of a bumpy structure is to use analogies of the mechanism of incubation effect in laser-induced damage threshold. The incubation effect is that the laser-induced damage threshold can be changed depending on the pulse train condition, such as the number of pulses per area and the time interval between laser pulses (pulse repetition rate of the laser). According to Sun et al. (Sun, Lenzner, and Rudolph 2015), the incubation effect occurs through two different mechanisms. One is absorption changes caused by the formation of surface ripples. Another one is critical energy changes caused by heat accumulation. According to the results from Sun et al. (Sun, Lenzner, and Rudolph 2015), the dominance of either mechanism can be changed by changing the time interval of pulses at the same spatial pulse overlap.

In this study, aiming to create a bumpy structure on thin metal films, morphologies created at different heat accumulation conditions were examined. The heat accumulation was controlled by changing the time interval between laser pulses (1 µs, 2.5 µs, and 25 µs) and their peak fluence (pulse energy), while maintaining a constant spatial pulse overlap. In addition, the boundary of the growth mechanism of a bumpy structure is discussed by the incubation model. Therefore, it is investigated which incubation mechanism is dominant for different time intervals between the applied laser pulses.

2. Experiment

In this study, stainless steel sheets (SUS 304L, Hans-Erich Gemmel & Co. GmbH) with a dimension of 50x50 mm^2 were used. As a first step, a 1 mm thick sample was chosen to exclude the effect of bending due to heat accumulation and to focus only on surface morphology. Before and after the laser process, the sample was cleaned with isopropyl alcohol.

The samples were micro-structured with an ultra-short pulse (USP) laser system (Hyper-Rapid 100, Coherent Kaiserslautern GmbH) with a pulse duration of 10 ps and a wavelength of 532 nm. The laser system was integrated into a high-precision 5-axes micro-machining workstation equipped with a galvanometric scanner system. For the experiments, a telecentric F-Theta optic with a focal length of 100 mm was used, resulting in a spot diameter in the focal plane is 9.7 µm. The laser processing was done in ambient air. The laser-processed areas have a size of 1x1 mm^2.

To divide the effect of heat accumulation and other effects, the time interval and the peak fluence (pulse energy) have been varied.

The time interval of pulses is changed by changing the pulse repetition rate of the laser. The range of the pulse repetition rate was chosen from the calculation results of the time profile of the temperature at the center point of the beam after a single Gaussian pulse is irradiated on the surface. Figure 1 shows the time profile of increased temperature (ΔT) at the center point of the beam after a single Gaussian pulse is irradiated on the surface at two different pulse energies. The light blue horizontal line is the range of temperature where loses the strength of stainless steel (c.a. 300 K). Therefore, as one of the conditions to prevent heat accumulation, the time interval of pulses was set to 25 µs, which corresponds to the experimental condition of 40 kHz of the pulse repetition rate of the laser. On the other hand, if the time duration after the laser pulse is short, ΔT remains at a high temperature, even over the temperature when a significant loss in strength of stainless steel can be obtained. Therefore, as the experimental conditions with significant heat accumulation, 2.5 µs and 1 µs (as an extreme condition for it) were set, which correspond to the experimental condition of 400 kHz and 1000 kHz of pulse repetition rate. In order to see the effect of the time interval of pulses even in the same range of total energy per area, the number of pulses per area (or spatial pulse overlap) was kept the same at each pulse repetition rate by changing the scanning speed.

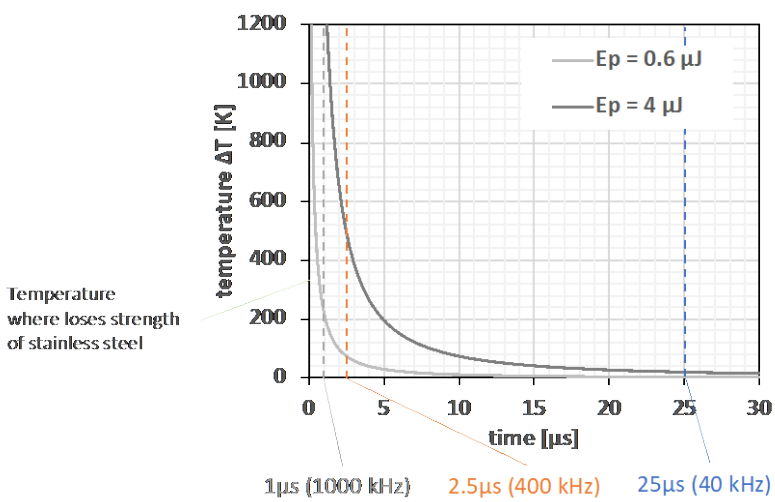

Fig. 1. The time profile of increased temperature from a single pulse irradiation at the center point of the beam

Additionally, according to figure 1, if the pulse energy is low, even at a short time interval of pulses, increased temperature ΔT is low. Therefore, to divide the heat accumulation condition and non-heat accumulation condition, various pulse energy (peak fluence) was also examined.

The variable experimental conditions are summarized in Table 1.

After creating the surfaces, the morphology of each prepared surface was measured by scanning electron microscopy (SEM).

Table 1. Experimental conditions for changing heat accumulation states

time interval of pulses	25 µs	2.5 µs	1 µs
pulse repetition rate of laser	40 kHz	400 kHz	1000 kHz
scan speed	100 mm/s	1000 mm/s	2500 mm/s
spatial pulse overlap		72.5 %	
peak fluence		0.4 to 30.6 J/cm^2	
scan number		1 to 101	

3. Results and discussion

The morphologies measured by SEM at different laser conditions are summarized in figure 2, 3, and 4 for time intervals of pulses of 1 µs, 2.5 µs, and 25 µs, respectively.

According to figure 2, 3, and 4, at all conditions with high peak fluence and high scan number, the bumpy structure appeared (red-colored area).

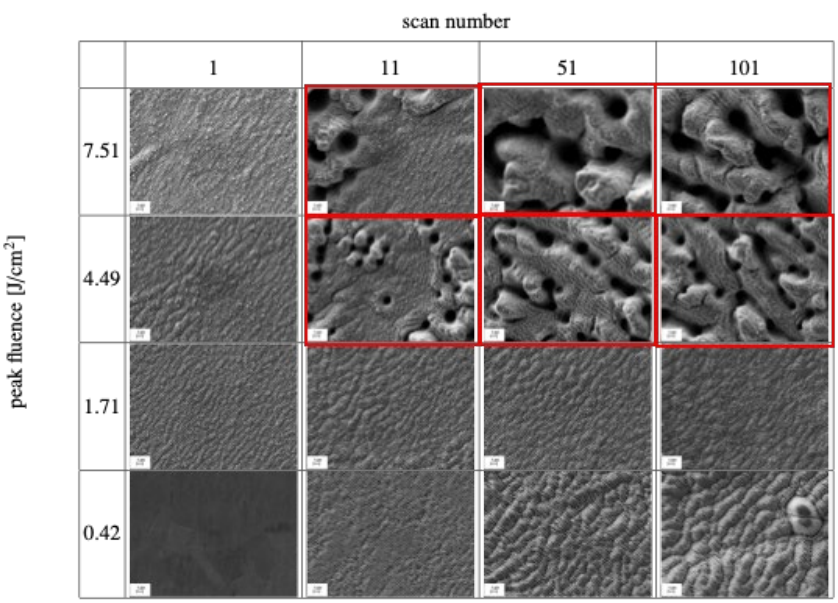

Fig. 2. The morphologies at various peak fluence and scan number: time interval of pulses is 1 µs.

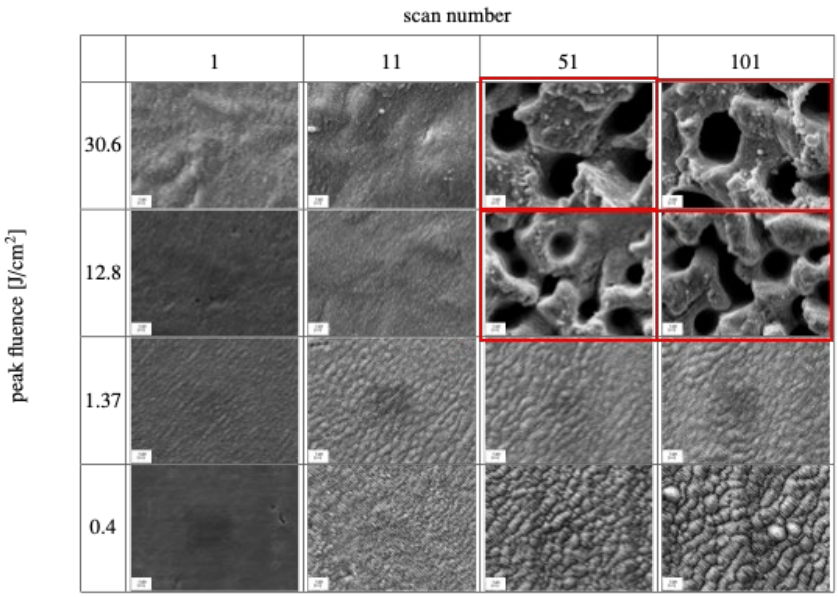

Fig. 3. The morphologies at various peak fluence and scan number: time interval of pulses is 2.5 µs.

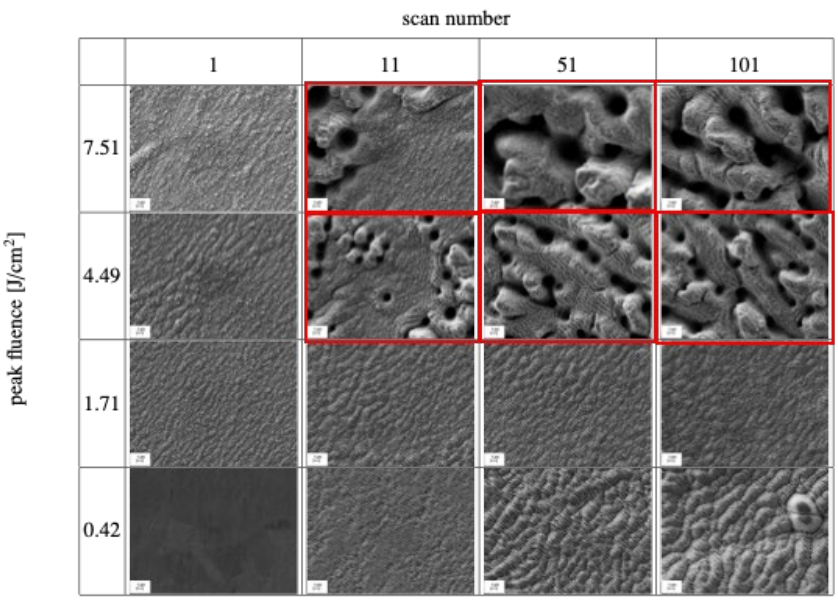

Fig. 4. The morphologies at various peak fluence and scan number: time interval of pulses is 25 µs.

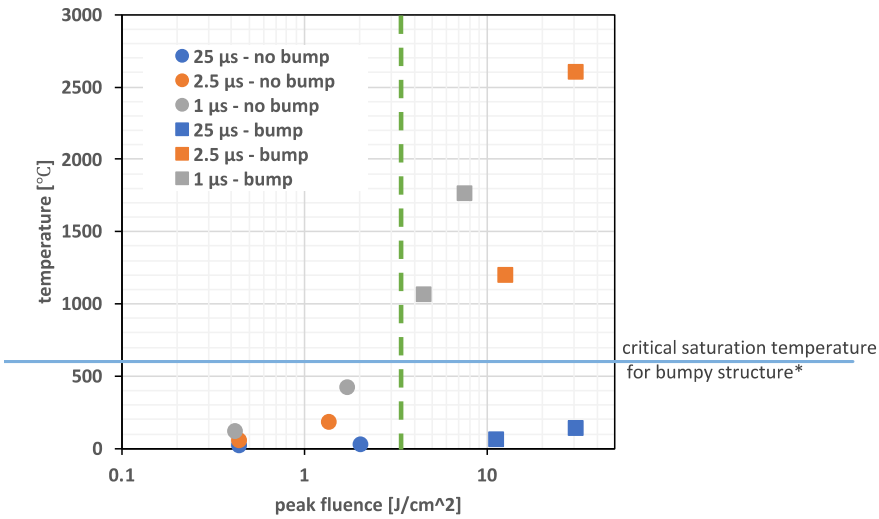

Fig. 5. The results of saturation temperature at each experimental condition. Circle (●) points show the condition for not bumpy structures, and square (■) points show the conditions for bumpy structures. *The critical saturation temperature for the bump is shown in the blue line and referred from the paper (Bauer et al. 2015).

To see the relationship between heat accumulation conditions and morphology, the saturation temperatures (T_{sat}) at the center point in the laser scanning area for each laser condition were calculated. To obtain saturation temperatures for each experimental condition, a model similar to the one described in Bauer et al. (Bauer et al. 2015) was used. Additionally, the critical saturation temperature for forming a bumpy structure at stainless steel (T_{crit}) was referred from the same paper and is set to 607 ℃.

Figure 5 shows the calculated results of saturation temperature at each laser condition. The blue horizontal line is the critical saturation temperature for bumpy structures. According to figure 5, for conditions of all time intervals of pulses, when the peak fluence is small (lower than the green vertical dashed line), there is no bumpy structure formed. On the other hand, in the high peak fluence range (higher than the green vertical dashed line), the bumpy structures were formed. However, the heat accumulation condition is different from each time interval of pulses' conditions. According to figure 5, the saturation temperature at the condition of the time interval of pulses of 1 μs and 2.5 μs exceeds the critical saturation temperature for bumpy structures. However, the saturation temperatures at the conditions with the time interval of pulses of 25 μs do not exceed the critical saturation temperature for bumpy structures. These results suggest that there is another explanation is needed for the formation of the bumpy structure instead of critical saturation temperature. According to figure 2, when the bumpy structure at the time interval of pulses of 25 μs is compared to the one at time interval of pulses of 2.5 μs and 1 μs, lots of debris on top of the bumpy structure can be seen at the time interval of pulses of 25 μs. On the other hand, there is less debris, and LIPSS can be seen on the top of the bumpy structure at time interval of pulses of 2.5 μs and 1 μs. This result suggests that the growth mechanism of a bumpy structure is different at the time interval of pulses of 25 μs and at the time interval of pulses of 2.5 μs and 1 μs. For the future, further experiments are needed, for example, the cross-section image cut by a focused ion beam (FIB), and then the oxidation states of bumpy structures are needed to be studied.

The effect of the time interval of pulses in the mechanism of how laser interacts with the sample surface is also discussed in the incubation effect. As it is described in the introduction section, this incubation mechanism has analogies with the growth mechanism of a bumpy structure. Therefore, one of the hints for discussing the

boundary of the growth mechanism of a bumpy structure might be the incubation effect in different time interval of pulses' conditions.

Therefore, which incubation mechanism is dominant at the different time interval of pulses is studied. To obtain the dominance of the incubation mechanism, the equation from Sun et al. (Sun, Lenzner, and Rudolph 2015) was used (shown in equation 1).

$$F_{th,Sun(N_a)} = \frac{F_{th,N_a=1} - \left[F_{th,N_a=1} - F_{th,N_a\to\infty}\left(1+\frac{\alpha}{\alpha_0}\right)\right]\left[1-e^{-\gamma F(N_a-1)}\right]}{1+\frac{\alpha}{\alpha_0}\left[1-e^{-\beta F(N_a-1)}\right]} \quad (1)$$

where N_a is the number of pulses per area, $F_{th,\,N_a=1}$ is the damage threshold at a single pulse, $F_{th,\,N_a\to\infty}$ is the damage threshold at high numbers of pulses per area, α is the absorption coefficient during pulse train, α_0 is initial absorption coefficient, γ is a coefficient for the pulse induced change of critical energy density, β is a coefficient for the pulse induced change of absorption coefficient.

When the experimental results are fitted by equation 1, fitting parameters are α/α_0, γ and β. When $\gamma > \beta$, the incubation mechanism is absorption dominant, and when $\gamma < \beta$, the incubation mechanism is heat accumulation dominant.

Therefore, the laser-induced damage threshold at each time interval of pulses conditions is obtained by the method given by Liu et al. (Liu 1982). In order to obtain fitting parameters in equation 1, the laser-induced damage thresholds for different numbers of pulses per area were examined. In this experiment, the number of pulses per area was varied by changing the scan speed, as shown in equation 2.

$$N_a = \frac{1}{1-\frac{PO}{100}} \quad (2)$$

where *PO* is spatial pulse overlap. The detail of the experimental condition is summarized in table 2.

Table 2. Experimental conditions for laser damage threshold

time interval of pulses	25 µs	2.5 µs	1 µs
pulse repetition rate	40 kHz	400 kHz	1000 kHz
number of pulses per area (spatial pulse overlap)	1 to c.a. 1000 (single, PO 56 % to 99.9 %)		
peak fluence	0 to over 10 J/cm^2		

The results of damage threshold vs number of pulses per area at the different time intervals of pulses' conditions are shown in figure 6. The experimentally obtained data were fitted with equation 1. The parameter values, found by fitting, are shown in Table 3. According to table 3, only for the time interval of 25 µs, γ is larger than β. In this time interval range, the dominant incubation mechanism is absorption. While, at time intervals of 2.5 µs and 1 µs, γ is smaller than β. Therefore, in this time interval range, heat accumulation the dominant incubation mechanism.

The trend in the difference in the dominance of the incubation mechanism is the same as the trend in the difference of saturation temperature (below or above critical saturation temperature). Therefore, the results promote the idea that the boundary of the growth mechanism for forming bumpy structures might be predictable by the incubation model. For a better understanding of the mechanism of creating a bumpy structures without significant heat accumulation, further experiments are needed.

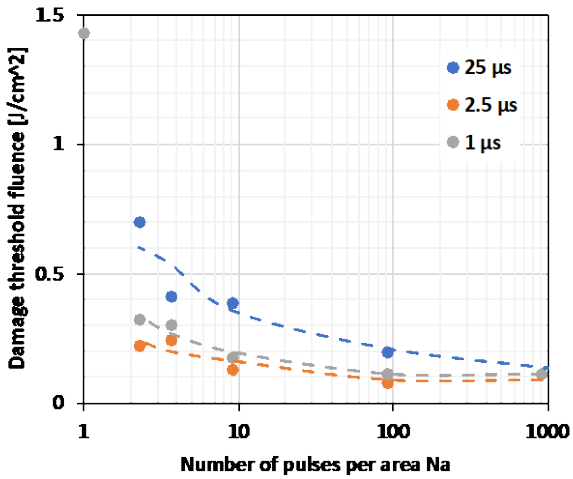

Fig. 6. The results of laser-induced damage threshold at different numbers of pulses per area. Experimental data (dots) are fitted with the incubation model from Sun et al. (Sun, Lenzner, and Rudolph 2015) (dashed line)

Table 3. The results of fitting parameters in the model based on Sun et al.(Sun, Lenzner, and Rudolph 2015).

time interval of pulses	25 µs	2.5 µs	1 µs
$\Delta\alpha/\alpha 0$	2.29	3.95	2.17
γ	1.77 cm^2/J	0.92 cm^2/J	0.97 cm^2/J
β	0.04 cm^2/J	80.5 cm^2/J	80.5 cm^2/J
	$\gamma > \beta$	$\gamma < \beta$	$\gamma < \beta$

4. Conclusion

Aiming to create a bumpy structure on thin metal films with low heat accumulation, in this study morphologies at different heat accumulation conditions were examined, by changing the time interval between laser pulses (1 µs, 2.5 µs and 25 µs) and the peak fluence (pulse energy) while maintaining a constant spatial pulse overlap. The saturated temperature was calculated by the model based on Bauer et al.(Bauer et al. 2015).

The comparison of morphologies and calculated saturation temperature shows that with a high peak fluence, there are conditions where bumpy structures are formed, even below the critical saturation temperature for bumpy structures. This result suggests that the growth mechanism of bumpy structures is different for short (2.5 µs and 1 µs) and long (25 µs) time intervals between lasers pulses.

To discuss the boundary of the growth mechanism of bumpy structure, using analogies in the mechanism of incubation effect in laser-induced damage threshold, which incubation mechanism is dominant at the different time interval of pulses is studied. The analysis from the incubation model based on Sun et al. (Sun, Lenzner, and Rudolph 2015) showed that only the condition at the time interval of pulses of 25 µs, the incubation mechanism is the absorption dominant and other condition at the time interval of pulses of 2.5 µs and 1 µs is heat accumulation dominant.

The trend in the difference in the dominance of the incubation mechanism is the same as the trend in the difference in saturation temperature (below or above critical saturation temperature). Therefore, the results

promote the idea that the boundary of the growth mechanism of a bumpy structure might be predictable by the incubation model.

For a better understanding of the growth mechanism of a bumpy structure without significant heat accumulation, further experiments are needed.

Acknowledgements

This project was supported by Deutsche Forschungsgemeinschaft project number 467661067.

References

C. A. Zuhlke, T. P. Anderson, and D. R. Alexander, "Formation of multiscale surface structures on nickel via above surface growth and below surface growth mechanisms using femtosecond laser pulses," Opt Express, vol. 21, no. 7, pp. 8460–8473, Apr. 2013, doi: 10.1364/OE.21.008460

C. Pence, H. Ding, N. Shen, and H. Ding, "Experimental analysis of sheet metal micro-bending using a nanosecond-pulsed laser," Int. J. Adv. Manuf. Technol., vol. 69, no. 1, pp. 319–327, Oct. 2013, doi: 10.1007/s00170-013-5032-8.

C. Schönecker, T. Baier, and S. Hardt, "Influence of the enclosed fluid on the flow over a microstructured surface in the Cassie state," J. Fluid Mech., vol. 740, pp. 168–195, 2014, doi: 10.1017/jfm.2013.647.

C. Sciancalepore, L. Gemini, L. Romoli, and F. Bondioli, "Study of the wettability behavior of stainless steel surfaces after ultrafast laser texturing," Surf. Coat. Technol., vol. 352, pp. 370–377, Oct. 2018, doi: 10.1016/j.surfcoat.2018.08.030.

E. J. Y. Ling, J. Saïd, N. Brodusch, R. Gauvin, P. Servio, and A.-M. Kietzig, "Investigating and understanding the effects of multiple femtosecond laser scans on the surface topography of stainless steel 304 and titanium," Appl. Surf. Sci., vol. 353, pp. 512–521, 2015, doi: https://doi.org/10.1016/j.apsusc.2015.06.137.

F. Bauer, A. Michalowski, T. Kiedrowski, and S. Nolte, "Heat accumulation in ultra-short pulsed scanning laser ablation of metals," Opt Express, vol. 23, no. 2, pp. 1035–1043, Jan. 2015, doi: 10.1364/OE.23.001035.

F. Fraggelakis, G. Mincuzzi, J. Lopez, I. Manek-Hönninger, and R. Kling, "Texturing metal surface with MHz ultra-short laser pulses," Opt Express, vol. 25, no. 15, pp. 18131–18139, Jul. 2017, doi: 10.1364/OE.25.018131.

F. Nyenhuis, P. N. Terekhin, T. Menold, B. Rethfeld, A. Michalowski, and J. A. L'huillier, "Fundamentals of Scanning Surface Structuring by Ultrashort Laser Pulses: From Electron Diffusion to Final Morphology," Adv. Photonics Res., vol. 3, no. 9, p. 2200045, 2022, doi: https://doi.org/10.1002/adpr.202200045.

G. Giannuzzi et al., "Short and long term surface chemistry and wetting behaviour of stainless steel with 1D and 2D periodic structures induced by bursts of femtosecond laser pulses," Appl. Surf. Sci., vol. 494, pp. 1055–1065, Nov. 2019, doi: 10.1016/j.apsusc.2019.07.126.

J. Yong, F. Chen, Q. Yang, J. Huo, and X. Hou, "Superoleophobic surfaces," Chem Soc Rev, vol. 46, no. 14, pp. 4168–4217, 2017, doi: 10.1039/C6CS00751A.

J. M. Liu, "Simple technique for measurements of pulsed Gaussian-beam spot sizes," Opt Lett, vol. 7, no. 5, pp. 196–198, May 1982, doi: 10.1364/OL.7.000196.

K. Manoharan and S. Bhattacharya, "Superhydrophobic surfaces review: Functional application, fabrication techniques and limitations," J. Micromanufacturing, vol. 2, no. 1, pp. 59–78, 2019, doi: 10.1177/2516598419836345.

K. M. T. Ahmmed, E. J. Y. Ling, P. Servio, and A.-M. Kietzig, "Introducing a new optimization tool for femtosecond laser-induced surface texturing on titanium, stainless steel, aluminum and copper," Opt. Lasers Eng., vol. 66, pp. 258–268, 2015, doi: https://doi.org/10.1016/j.optlaseng.2014.09.017.

M. Martínez-Calderon, A. Rodríguez, A. Dias-Ponte, M. Morant-Miñana, M. Gómez-Aranzadi, and S. Olaizola, "Femtosecond laser fabrication of highly hydrophobic stainless steel surface with hierarchical structures fabricated by combining ordered microstructures and LIPSS," Appl. Surf. Sci., vol. 374, pp. 81–89, 2016.

N. Berger et al., "Friction reduction of stainless steel surfaces by laser microstructuring," in Friction reduction of stainless steel surfaces by laser microstructuring, Wissenschaftlichen Gesellschaft Lasertechnik e.V., 2021.

S. Faas, U. Bielke, R. Weber, and T. Graf, "Prediction of the surface structures resulting from heat accumulation during processing with picosecond laser pulses at the average power of 420 W," Appl. Phys. A, vol. 124, no. 9, p. 612, Aug. 2018, doi: 10.1007/s00339-018-2040-4.

Z. Sun, M. Lenzner, and W. Rudolph, "Generic incubation law for laser damage and ablation thresholds," J. Appl. Phys., vol. 117, no. 7, p. 073102, 2015.